Scientific paper

Simplified Inverse Method for Determining the Tensile Strain Capacity of Strain Hardening Cementitious Composites

Shunzhi Qian[1] and Victor C. Li[2]

Received 11 December 2006, accepted 27 April 2007

Abstract

As emerging advanced construction materials, strain hardening cementitious composites (SHCCs) have seen increasing field applications recently to take advantage of its unique tensile strain hardening behavior, yet existing uniaxial tensile tests are relatively complicated and sometime difficult to implement, particularly for quality control purpose in field applications. This paper presents a new simple inverse method for quality control of tensile strain capacity by conducting beam bending test. It is shown through a theoretical model that the beam deflection from a flexural test can be linearly related to tensile strain capacity. A master curve relating this easily measured structural element property to material tensile strain capacity is constructed from parametric studies of a wide range of material tensile and compressive properties. This proposed method (UM method) has been validated with uniaxial tensile test results with reasonable agreement. In addition, this proposed method is also compared with the Japan Concrete Institute (JCI) method. Comparable accuracy is found, yet the present method is characterized with much simpler experiment setup requirement and data interpretation procedure. Therefore, it is expected that this proposed method can greatly simplify the quality control of SHCCs both in execution and interpretation phases, contributing to the wider acceptance of this type of new material in field applications.

1. Introduction

In the past decade, great strides have been made in developing strain hardening cementitious composite (SHCC), characterized by its unique macroscopic pseudo strain hardening behavior after first cracking when it is loaded under uniaxial tension. SHCCs, also referred to as high performance fiber reinforced cementitious composites (HPFRCCs, Naaman and Reinhardt 1996), develop multiple cracks under tensile load in contrast to single crack and tension softening behavior of concrete and conventional fiber reinforced concrete. Multiple cracking provides a means of energy dissipation at the material level and prevent catastrophic fracture failure at the structural level, thus contributing to structural safety. Meanwhile, material tensile strain hardening (ductility) has been gradually recognized as having a close connection with structural durability (Li 2004) by suppressing localized cracks with large width. Many deterioration and premature failure of infrastructure can be traced back to the brittle nature of concrete. Therefore, SHCCs are considered as a promising material solution to the global infrastructure deterioration problem and tensile ductility is the most important property of this type of material.

[1]Research Assistant, Department of Civil and Environmental engineering, University of Michigan, USA.
[2]Professor, Department of Civil and Environmental engineering, University of Michigan, USA.
E-mail: vcli@umich.edu

Engineered Cementitious Composites (ECC, Li 1993) is a unique representative of SHCCs, featuring superior ductility (typically > 3%, 300 times that of normal concrete or FRC) (Li and Kanda 1998; Li *et al* 2001), tight crack width (less than 80μm, Li 2003), and relatively low fiber content (2% or less of short randomly oriented fibers). A typical tensile stress-strain curve of ECC is shown in **Fig. 1**. It attains high ductility with relatively low fiber content via systematic tailoring of the fiber, matrix and interface properties, guided by micromechanics principles. Enhanced with such high tensile ductility and/or tight crack width, ECC has demonstrated superior energy dissipation capacity, high damage tolerance, large deformation capacity, and exceptional durability in many recent experimental investigations (Li 2005). As a result, ECC is now emerging in the field and has seen increasing infrastructure applications, such as dam repair, bridge deck overlay and link slab, coupling beam in high-rise building, and other structural elements and systems (Li 2004).

As aforementioned, tensile ductility is the most important material property of SHCC, yet relatively large variation of tensile ductility was observed in the literature (Kanda *et al* 2002, 2006; Wang and Li 2004). To address such concern, Wang and Li (2004) have proposed using artificial flaws with prescribed size distribution as defect site initiator to create more saturated multiple cracks, resulting in more consistent tensile strain capacity among different specimens from the same batch. The overall tensile strain capacity shows much more consistent results after implantation of artificial flaws, however, the variation of tensile strain capacity is still relatively large when compared with that

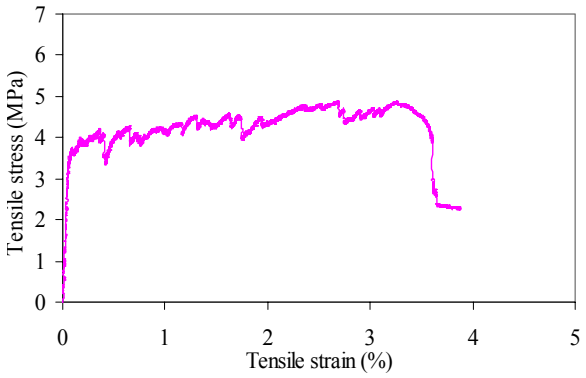

Fig. 1 Typical tensile stress-strain curve of ECC.

of other properties, e.g., first cracking strength. Therefore, test method for quality control of SHCCs onsite should logically focus on tensile strain capacity due to its importance in governing structural response and potentially large variability.

While most characterization of the tensile behavior of SHCCs was carried out using uniaxial tensile test (UTT) in academia, this method is generally considered to be complicated, time-consuming and require advanced equipment and delicate experimental skills. Therefore, it is not suitable for onsite quality control purpose (Stang and Li 2004, Ostergaard *et al* 2005, Kanakubo 2006). First, special fixtures and/or treatments for the ends of specimens are usually needed in order to transfer tensile loads. Furthermore, the specimen is sensitive to stress concentration induced by misalignment and can fail near the end prematurely. Last but not least, realistic dimensions for specimens large enough to have 3-dimensional random fiber orientation make the UTT even more difficult to conduct.

As a simpler alternative to the UTT, four point bending test (FPBT) was proposed by Stang and Li (2004) for quality control on construction sites, provided that an appropriate interpretation procedure for the test result is available. FPBT, in which the mid-span of the specimen undergoes constant bending moment, may be carried out to determine the moment-curvature or moment-deflection curves. This type of test is much easier to set up and conduct in comparison to UTT, and a large amount of experience in bending test has been accumulated in the user community of cementitious materials. The ultimate goal of this test is to use the moment-curvature or moment-deflection curves so determined to invert for the uniaxial tensile properties. It should be noted, however, that the bending test is not meant to determine whether the material has tensile strain-hardening behavior or tension-softening behavior, but rather to constrain the tensile material parameters, e.g. the tensile strain capacity, as part of the quality control process in the field.

Inverse analyses for FPBT have recently been attempted by Technical University of Denmark (DTU) and Japan Concrete Institute (Ostergaard *et al* 2005; Kanakubo 2006) with certain success. By adopting a simplified elastic-perfectly plastic tensile model, JCI method generally can predict plateau tensile strength and tensile strain capacity from the FPBT results via a sectional analysis similar to that developed by Maalej and Li (1994). On the other hand, hinge model, including both tensile strain hardening and tension softening effect, was employed in the DTU inverse method along with least square method to invert for tensile material properties from their bending response. The model can predict experimental load – deflection curve fairly well and tensile properties derived based on this method agree well with that from FEM analysis, yet no direct comparison with UTT results has been made so far.

Despite the successes mentioned above, further simplification and/or validation are necessary to make the FPBT widely accepted for quality control of SHCCs. In case of JCI method, significant improvement is needed to simplify the experimental execution and data interpretation procedure. For instance, LVDTs are required in JCI method to measure the beam curvature. This is somewhat burdensome in field conditions, considering quality control may involve a large number of specimens. Furthermore, the inverse process is not user friendly, which require relatively complicated calculation (solving cubic equation). As for the DTU method, firstly it needs complementary UTT results to truly validate the model. Secondly, the uniqueness of solution from such inverse analysis is questionable at times. Finally, the method will need to be packaged into sophisticated software, which may incur additional user cost. A simple engineering chart with reasonable accuracy may be more preferable.

Keeping these considerations in mind, this paper looks to develop a greatly simplified yet reasonably accurate inverse method for determining tensile strain capacity of SHCCs. In the following sections, the research significance and overall research framework for the proposed method will be presented first, followed by parametric study to obtain the master curves for inverse analysis. Thereafter, the experimental program consisting of both FPBT and complementary UTT will be revealed in detail. The results from FPBT will then be converted to tensile strain capacity and validated with independent UTT test results. Finally, the proposed method will be compared with JCI inverse method, followed by overall conclusions.

2. Overall research framework

The overall research framework is revealed in **Fig. 2**, consisting of detailed procedure for development and execution of inverse method (top frame (a)) and validation and verification procedure (bottom frame (b)). As shown in the top frame (a), deflection capacity (deflection corresponding to peak bending stress, i.e., modulus of rupture) can be obtained from FPBT. By conducting

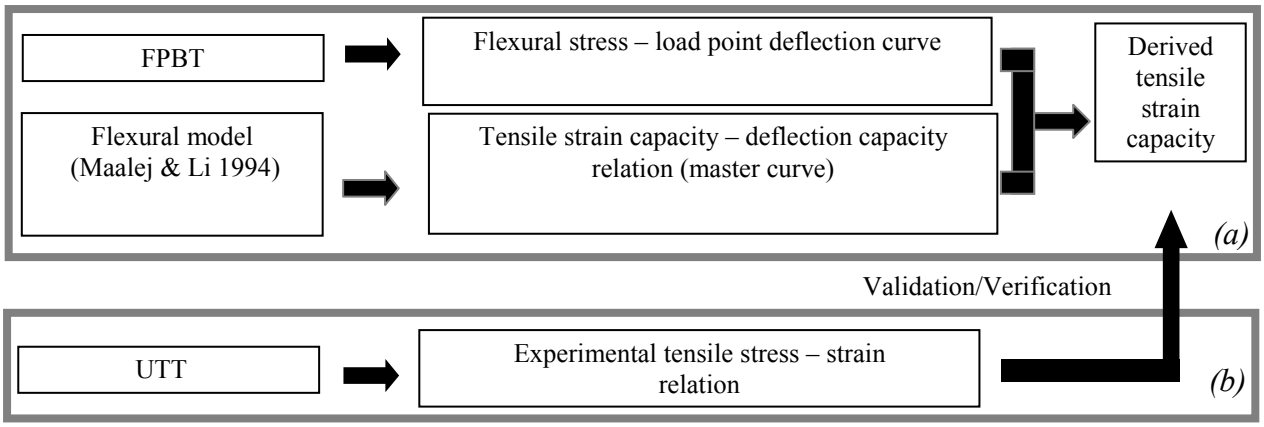

Fig. 2 Overall research framework for proposed UM method.

parametric studies based on a flexural behavior model of SHCCs, master curve can be constructed in terms of tensile strain capacity with respect to deflection capacity. Based on deflection capacity of FPBT and master curve from parametric study, tensile strain capacity of SHCCs can be derived. Additionally, companion UTT test using specimens cast from the same batch of material is used to validate and/or verify the proposed method in terms of the accuracy of derived tensile strain capacity, which is shown in bottom frame (b). It is conceived that a large number of FPBT will be conducted at construction sites on daily basis to ensure the quality of the SHCC material. The extra step of verification (Frame (b)) will not be necessary once the method is standardized and utilized in practice, except a very limited number of UTT specimens to be cast onsite and tested at advanced research laboratory to check whether this material is truly a strain hardening type during trial mixing stage.

3. Parametric study and master curves

3.1 Flexural behavior model

The flexural behavior model used in this investigation is based on the work of Maalej and Li (1994). Compared with other models, the major distinction of this model is that the contribution of tensile strain hardening property of SHCCs was included. The actual SHCC considered in the model is Polyethylene ECC (PE-ECC) material. To simplify the analysis, the stress – strain behavior of the ECC was assumed as bilinear curves in both tension and compressive. Based on a linear strain profile and equilibrium of forces and moment in a section, the relation between flexural stress and tensile strain at the extreme tension fiber (Simplified as critical tensile strain hereafter) can be determined as a function of basic material properties. Overall, the model predicts experimentally measured flexural response quite well. For more detail, the readers are referred to Maalej and Li (1994).

Based on geometrical considerations, the beam curvature can be computed as the ratio of critical tensile strain to the distance from the extreme tension fiber to the neutral axis. This can be expressed in following equation:

$$\phi = \frac{1}{\rho} = \frac{\varepsilon_t}{c} \tag{1}$$

where ϕ, ρ, ε_t, and c are beam curvature, beam radius of curvature, critical tensile strain, and the distance from the extreme tension fiber to the neutral axis.

In a FPBT of SHCC material, according to structural mechanics, we can obtain following equation to relate the deflection of the beam to the curvature at the load point and therefore critical tensile strain. The load point

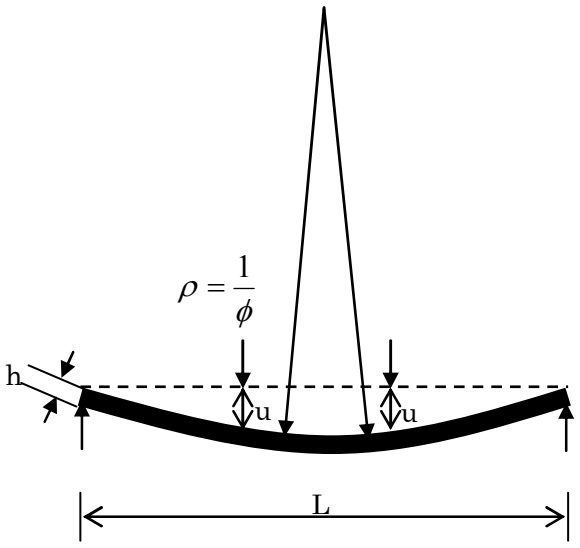

Fig. 3 Definition of load point displacement u, span length L, beam height h and curvature ϕ in a schematic FPBT test (curvature is constant along the middle third span between the two load points).

deflection for a beam with span length L is given by:

$$u = \frac{15 * \phi * L^2}{162} + \frac{\phi * L^2}{4}(\frac{h}{L})^2 \quad (2)$$

The definitions for u, ϕ, L and h are shown in **Fig. 3**. The first term includes the flexural deformation from pure bending span and shear span while the second term includes the shear deformation from shear span. It should be noted that the shear deformation is strongly related with the ratio of beam height over span length as shown in the second term. The specimens used in this study have a height and span length of 51mm, 305mm while corresponding values are 100mm and 300mm for JCI method. Therefore, the second term in Equation (2) for the UM method is at least an order of magnitude smaller than the first term, so that (2) can be simplified as follows:

$$u = 0.1 * \phi * L^2 \quad (3)$$

Since the relation between flexural stress and ε_t is already established, we can predict the flexural stress and load point deflection relation based on Equations (1) and (3). The maximum flexural stress (MOR) and corresponding deflection (deflection capacity) are reached once the strain capacity of the SHCCs is exhausted either at the extreme tensile fiber or at the extreme compression fiber, which is the assumed failure criterion in this model. The strain capacity is defined as tensile/compressive strain corresponding to ultimate tensile/compressive strength (maximum stress in stress-strain curve).

The model was originally developed based on material behavior of PE-ECC, it would be desirable to check its applicability for other SHCCs, such as PVA-ECC, which has been extensively investigated in the past decade. PVA-ECC 0, with mix proportion and material tensile and compressive properties shown in **Table 1**, was utilized to check the applicability of the model. As shown in **Fig. 4**, the analytical result from the model predicts the experimental flexural stress-deflection curves reasonably well, particularly in terms of average MOR and deflection capacity prediction. This seems to suggest that the model is quite versatile in predicting the flexural behavior of SHCCs.

3.2 Construction of master curves

Parametric study was conducted to investigate the influence of material uniaxial tensile and compressive properties (parametric values) on the flexural response of SHCCs based on the aforementioned flexural model. The correlation between tensile strain capacity and load point deflection was established and constructed as master curve. All tensile and compressive properties were varied within a wide range of parametric values (**Table 2**), covering the normal range of test results of SHCC specimens at UM and JCI (Kanakubo 2006). It is expected that the master curves based on this wide range of parametric study can be directly utilized for quality control purpose in field.

With material parameters shown in **Table 3**, five cases of parametric study were plotted in **Fig. 5** as examples. The material parameters varied in first cracking strength, ultimate tensile strength, modulus of elasticity and compressive strength compared with Case 1 in **Table 3**. **Figure 5** shows the flexural stress, load point

Table 1 Mix proportion and material properties of PVA-ECC 0.

Mix proportion						Material properties			
Cement	Sand	Fly Ash	Water	Super-plasticizer	Fiber	First cracking strength (MPa)	Ultimate tensile strength (MPa)	Tensile strain capacity (%)	Compressive strength (MPa)
1	1	0	0.44	0.007	0.02	5.1±0.2	5.7±0.5	2.0±1.0	50.7±5.3

Note: Mix proportion is by weight except PVA fiber by volume. The modulus of elasticity and the ultimate compressive strain are assumed to be 18 GPa and 0.005, respectively.

Table 2 Range of material parameters used in parametric studies to construct the tensile strain capacity – deflection capacity (curvature) relation.

	Tensile properties				Compressive properties	
Material parameters	First cracking strength (MPa)	Ultimate tensile strength (MPa)	Tensile strain capacity (%)	Modulus of elasticity (GPa)	Compressive strength (MPa)	Compressive strain capacity (%)
Range	2.5~13.0	4.0~16.0	0~5	12~53	31~200	0.5~1*

Note: Parameters are in the normal range of test results of SHCC specimens at UM and JCI; Tensile and compressive modulus of elasticity are assumed to be equal; Beam dimensions are 51x76x356mm/100x100x400mm with span length of 305mm/300mm for UM and JCI specimens, respectively; *: Estimated range.

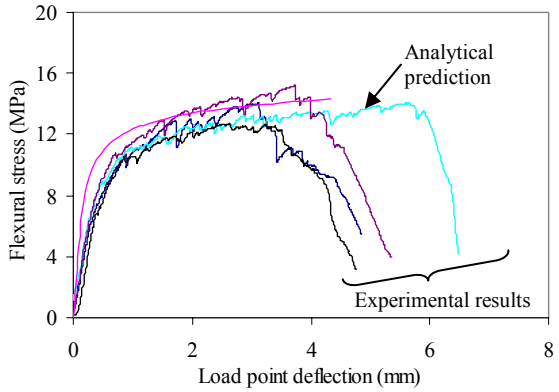

Fig. 4 Comparison of experimental results and analytical prediction of flexural stress-load point deflection for PVA-ECC 0.

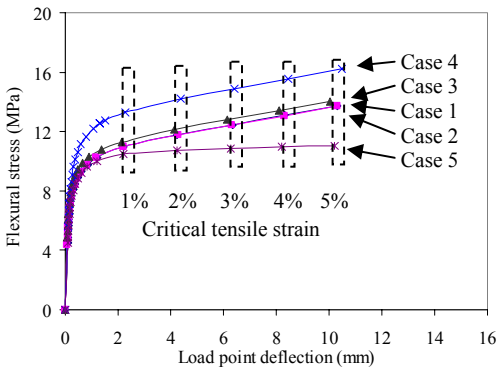

Fig. 5 Parametric study for SHCCs with different material parameters (Dashed line boxes include markers corresponding to same critical tensile strain (tensile strain at the extreme tension fiber); markers are plotted on 1% strain interval after 1% strain for all cases) (Notice Case 1 and Case 2 are almost coincided).

deflection and corresponding critical tensile strain relation. Beam dimensions are 51x76x356mm with span length of 305mm. From the Figure, load point deflections were observed to correlate very well with critical tensile strains, regardless of the actual parametric material properties. Once the critical tensile strain reaches the tensile strain capacity, the beam reaches peak load and the corresponding load point deflection is the deflection capacity. Therefore, it appears that the deflection capacity and tensile strain capacity can be linearly correlated regardless of the values of other material properties.

The overall results from the parametric study indeed show a linear relation between tensile strain capacity and deflection capacity, as revealed in **Fig. 6 (a)**. Totally 20 cases were investigated in the parametric study, with the range of material parameters shown in **Table 2**. All linear curves lie in a narrow band regardless of the values of other material properties, which suggests that the beam deflection capacity is most sensitive to tensile strain capacity for a fixed geometry. For ease of quality control on site, a master curve was constructed as a line with uniform thickness to cover all parametric case studies, as shown in **Fig. 6 (b)**. The top edge of the master curve is made to coincide with the upper boundary of all curves in **Fig. 6(a)** for conservativeness.

Additionally, another master curve correlating tensile strain capacity with curvature was constructed by parametric study in order to compare the proposed UM method with JCI method, in which ultimate bending moment and curvature was utilized to derive tensile strain capacity. The range of parametric values is the same as the aforementioned parametric study, as shown in **Table 2**. The dimension of specimen used in this parametric study is 100x100x400mm, with a span length of 300mm (JCI-S-003-2005).

As expected, this set of master curve also characterizes a linear relation within a very narrow band regardless of actual material properties (**Figs. 7 (a)** and **(b)**). Since curvature may be linearly correlated with deflection using Equation (2), this master curve can be easily transformed into tensile strain capacity to deflection capacity relation, even though the slope should be different from **Fig. 6** due to different dimensions used in the two parametric studies. In the case when specimens with different dimensions have to be used for quality control, e.g. due to different fiber length, a different set of master curve should be constructed.

Table 3 Assumed material properties for different cases of SHCCs.

	Tensile properties				Compressive properties	
	First cracking strength (MPa)	Ultimate tensile strength (MPa)	Tensile strain capacity (%)	Modulus of elasticity (GPa)	Compressive strength (MPa)	Compressive strain capacity (%)
Case 1	4.0	5.6	5%	18	50	0.005
Case 2	4.0	5.6	5%	20	50	0.005
Case 3	4.0	5.6	5%	18	75	0.005
Case 4	5.0	6.6	5%	18	50	0.005
Case 5	4.0	4.0	5%	18	50	0.005

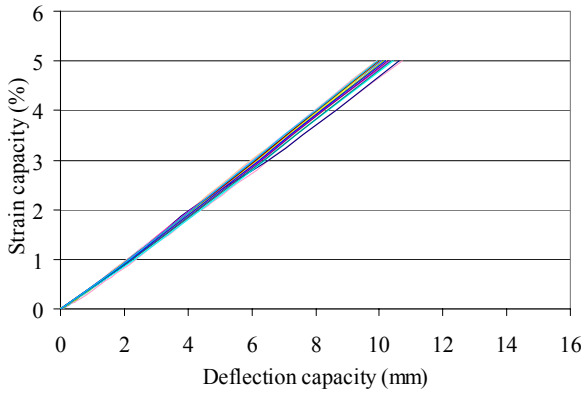

(a)

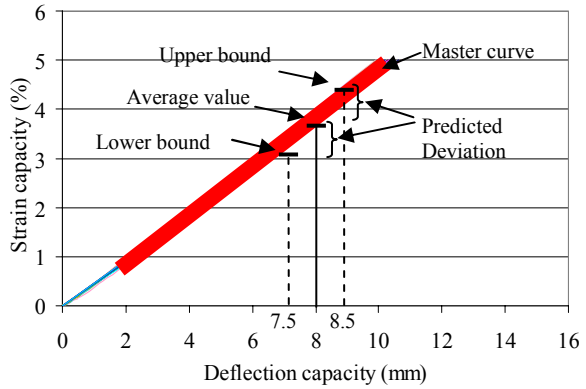

(b)

Fig. 6 (a) Tensile strain capacity –deflection capacity relation obtained from parametric study (20 cases); (b) Master curve transforming deflection capacity into tensile strain capacity.

3.3 Discussion on the unique behavior of master curves

The master curve reveals a linear behavior within a narrow band width. In the following, discussions will be presented to provide some understanding of this unique phenomenon.

As shown in Equations (1) and (2), for a given span length L, it can be observed that middle span deflection (u) and curvature (ϕ) would be linearly related to ε_t if c (the distance from extreme tension fiber to neutral axis) is constant with respect to ε_t. It turns out that this is approximately correct when ε_t is larger than 1%, as shown in **Fig. 8**, where parametric results are plotted for five cases of SHCCs (**Table 4**) in terms of distance from extreme tension fiber to neutral axis with tensile strain relation. It should be noted that the vertical axis (distance from extreme tension fiber to neutral axis) is normalized by the beam height.

On the other hand, it is observed that these normalized distance (normalized c value) near plateau are very close (ranging from 0.86 to 0.91) for cases with drastically different material properties. This explains the narrow band width of the master curve. The close plateau values for different cases may be due to the fact that most of the SHCC materials have a very high ratio between compressive strength and tensile strength, thus pushing the neutral axis very close to the extreme compressive fiber. Comparison between **Fig. 8** and **Table 4** suggests that the higher the ratio, the higher the normalized c value. Nevertheless, the small difference between these normalized c values suggests that narrow band width may characterize the master curve for most SHCC materials, in which ratio of compressive strength over tensile strength is about 10.

3.4 Use method of master curves

Based on the master curves obtained from parametric study, the deflection capacity from simple beam bending test can be easily converted to material tensile strain capacity, with detailed procedure schematically shown in **Fig. 6 (b)** and explained below. Assuming a deflection capacity of 8 mm with standard deviation of 0.5 mm already known from FPBT, the predicted average tensile strain capacity can be derived by taking the averaged strain value corresponding to 8 mm deflection. The

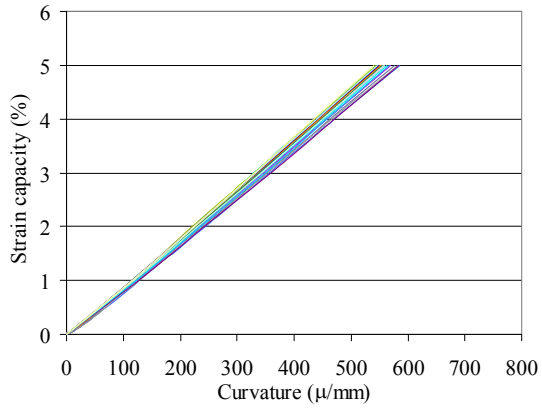

(a)

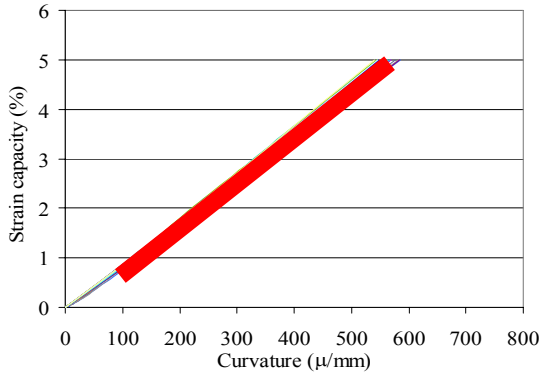

(b)

Fig. 7 (a) Tensile strain capacity –curvature capacity relation obtained from parametric study (20 cases); (b) Master curve transforming curvature capacity into tensile strain capacity.

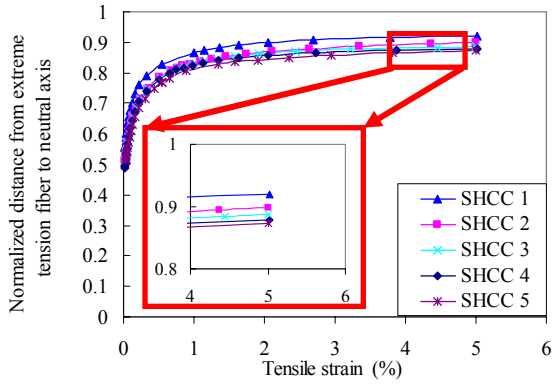

Fig. 8 Normalized distance from extreme tension fiber to neutral axis – tensile strain relation for SHCCs (distance normalized by the beam height).

upper and lower bound of the predicted tensile strain capacity can be obtained by taking maximum or minimum strain value corresponding to 8.5 mm or 7.5 mm deflection, respectively. The predicted deviation of tensile strain capacity is simply the difference between the upper/lower bound and average value.

A set of equations has been developed to simplify the conversion procedure, as shown below, where Equations (4) and (5) can be used to calculate the average tensile strain capacity and its deviation, respectively.

$$\varepsilon_{tu}^{'} = 0.50 \cdot \delta_u - 0.22 \tag{4}$$

$$PD = 0.50 \cdot SD + 0.18 \tag{5}$$

where $\varepsilon_{tu}^{'}$ is the predicted average tensile strain capacity (%); $\delta_u^{'}$ is the average deflection capacity obtained from FPBT (mm) (In **Fig. 6 (b)**, δ_u is assumed to be 8mm); *PD* is the predicted deviation for tensile strain capacity (%) considering the standard deviation of the deflection capacity, as shown in **Fig. 6(b)** and *SD* is the standard deviation of the deflection capacity (mm) (assumed to be 0.5 mm). To be conservative, the lower bound equals to the lowest strain capacity value corresponding to $\delta_u - SD$, which is assumed to be 7.5mm. Likewise, the upper bound equals to the highest strain capacity value corresponding to $\delta_u + SD$ (assumed to be 8.5mm). Therefore, the Predicted Deviation is the difference of upper bound/lower bound with predicted average tensile strain capacity.

It should be noted that this equation can only be applied to specimen with the same geometry and same loading conditions as that used by the authors (see Experimental Program section). Should any of these geometry and/or loading conditions change, another set of master curves and corresponding conversion equations should be developed for that purpose. Once the proposed method (or its modified version) is standardized and widely accepted, there should be no need for change in geometry and loading conditions.

A similar procedure can also be used to convert the curvature to strain capacity for the specimens tested according to the JCI method. A set of equation has also been developed according to **Fig. 7** to simplify the conversion procedure. Equations (6) and (7) can be used to calculate the average tensile strain capacity and its deviation, respectively.

$$\varepsilon_{tu,c} = 0.0093 \cdot \phi_{u,c} - 0.24 \tag{6}$$

$$PD_c = 0.0093 \cdot SD_c + 0.19 \tag{7}$$

where $\varepsilon_{tu,c}$ is the predicted average tensile strain capacity (%); $\phi_{u,c}$ is the average curvature capacity obtained from FPBT (μ/mm); PD_c is the predicted deviation for tensile strain capacity (%) and SD_c is the standard deviation of the curvature capacity (μ/mm). The same limitation as mentioned above for Equations (4) and (5) also applies to Equations (6) and (7), except that the specimen geometry and loading profile should follow those in the JCI method.

4. Experimental program

4.1 Materials, Specimen Preparation and Testing

The mix proportion of SHCC materials investigated in

Table 4 Comparison of ratio of compressive strength over average tensile strength for different SHCCs (material properties are assumed parametric values).

	Modulus of Elasticity (GPa)	First cracking strength (MPa)	Ultimate tensile strength (MPa)	Average tensile strength (MPa)	Comp. strength (MPa)	Ratio of comp. strength/Average tensile strength
SHCC 1	53	9.4	12.4	10.9	200	18.3
SHCC 2	18	4.0	4.0	4.0	50	12.5
SHCC 3	18	4.0	5.6	4.8	50	10.4
SHCC 4	14	2.5	4.2	3.35	31	9.3
SHCC 5	18	5.0	6.6	5.8	50	8.6

Note: All data are assumed values, in the normal range of test results at UM and the JCI round robin tests (Kanakubo 2006). For all cases, tensile and compressive strain capacity are assumed to be 5% and 0.5%.

this study is shown in **Table 5**, including PVA-ECC 1, 2 and 3. These SHCC materials feature high amount of fly ash in the mix proportion, with fly ash to cement ratios of 1.2, 2.0, and 2.8, respectively. Additionally, PVA-ECC 4 and Ductal from JCI round robin test (Kanakubo 2006) are also listed in **Table 5**, which will be used for comparison between UM method and JCI method.

A Hobart mixer was used in this investigation, with a full capacity of 12 liters. All beam, uniaxial tensile and compressive specimens were cast from the same batch. The beam and uniaxial tensile specimens were cast horizontally and compressive cylinder specimens were cast vertically. At least 3 specimens were prepared for each test. After demolding, all specimens were cured in a sealed container with about 99% humidity under room temperature for 28 days before testing.

Four point bending test was conducted with a MTS 810 machine. The beam specimen has a dimension of 356mm long, 50 mm high, and 76 mm deep, all dimensions are more than 5 times that of the PVA fiber length (8mm), which is the largest length scale among the ingredients of PVA-ECC. The loading span between two supports is 305mm with a constant moment span length of 102mm. The beam was tested under displacement control at a loading rate of 0.02 mm/second. The flexural stress was derived based on simple elastic beam theory and the beam deflection at the loading points was measured from machine displacement directly. The test setup is shown in **Fig. 9 (a)** in comparison with the JCI method (**Fig. 9 (b)**).

As shown in **Fig. 10**, uniaxial tensile test (UTT) was also carried out to directly verify the derived tensile strain capacity from four point bending test. The coupon specimen used herein measured 304.8 x 76.2 x 12.7 mm. Aluminum plates were glued at both ends of the coupon specimen to facilitate gripping (both ends are fixed). Tests were conducted in an MTS 810 machine with a 25 kN capacity under displacement control, with a loading rate of 0.0025mm/second throughout the test. Two external linear variable displacement transducers (LVDTs) were attached to specimen surface with a gage length approximately 180mm to measure the displacement.

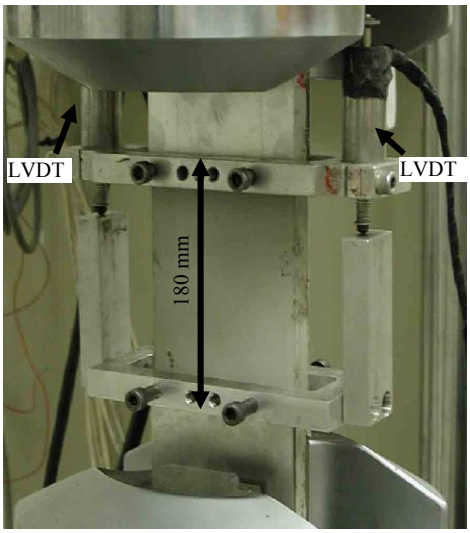

Fig. 10 Setup for uniaxial tensile test.

4.2 Experimental results

The material tensile and compressive properties for dif-

Table 5 Mix proportion for different SHCCs.

	Cement	Sand	Fly ash	Water/cementitious materials	Superplasticizer	Fiber
PVA-ECC 1	1	0.8	1.2	0.27	0.013	0.02
PVA-ECC 2	1	1.1	2	0.26	0.014	0.02
PVA-ECC 3	1	1.4	2.8	0.26	0.016	0.02
PVA-ECC 4*	-	-	-	0.46	-	0.019
Ductal*	-	-	-	0.22	-	0.02

Note: *: Data from JCI round robin test (Kanakubo, 2006)

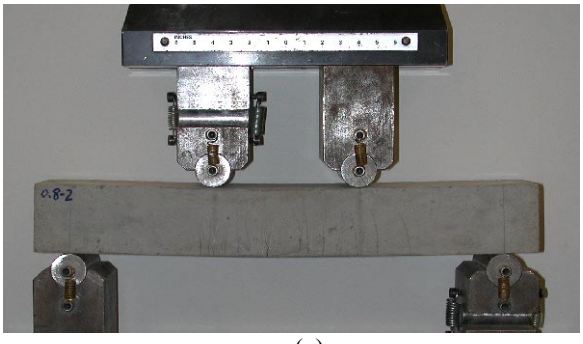

(a)

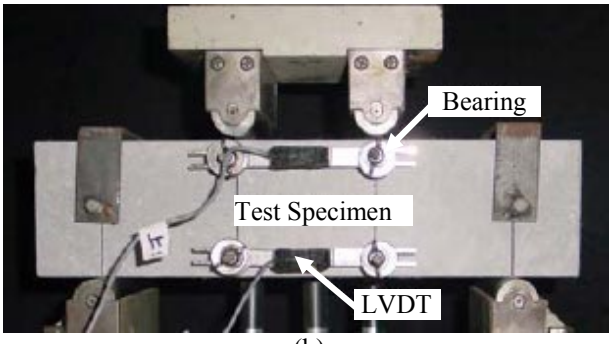

(b)

Fig. 9 Comparison of test setup for the (a) UM method and (b) JCI method (Beam deflection at the loading points was obtained from machine displacement directly in UM method).

Table 6 Material tensile and compressive properties from experiment for different SHCCs.

	First cracking strength (MPa)	Ultimate tensile strength (MPa)	Tensile strain capacity (%)	Compressive strength (MPa)
PVA-ECC 1	4.6±0.3 (7%)	5.3±0.6 (11%)	2.1±1.1 (52%)	54.6±6.5 (12%)
PVA-ECC 2	3.9±0.5 (13%)	4.6±0.2 (4%)	3.5±0.3 (9%)	46.0±3.8 (8%)
PVA-ECC 3	4.0±0.2 (5%)	4.9±0.1 (2%)	3.7±0.4 (11%)	37.5±1.7 (5%)
PVA-ECC 4*	3.7±0.8 (21%)	5.0±0.5 (10%)	2.7±0.7 (26%)	31.3±0.8 (3%)
Ductal*	13.7±0.9 (7%)	15.3±1.0 (7%)	0.5±0.3 (60%)	198.0±3.7 (2%)

Note: *: Experimental data from JCI round robin test (Kanakubo, 2006); Number in parenthesis is coefficient of variation (COV).

Table 7 Comparison between predicted tensile strain capacity from FPBT and tensile strain capacity from UTT.

	Tensile strain capacity from UTT (%)	Deflection capacity from FPBT (mm)	Predicted tensile strain capacity (%)	Difference between prediction and test result (%)
PVA-ECC 1	2.1±1.1	5.8±1.6	2.4±0.8	14%
PVA-ECC 2	3.5±0.3	7.0±1.3	3.3±0.5	-6%
PVA-ECC 3	3.7±0.4	9.3±0.9	4.4±0.1	19%

ferent SHCCs can be found in **Table 6**. With increasing amount of fly ash in PVA-ECC 1-3, the compressive strength continues to decrease as expected, yet PVA-ECC 3 still has a compressive strength of about 38 MPa. For all SHCCs the typical coefficient of variations (COV) of first cracking strength and ultimate tensile strength are less than 15%, similar to that of compressive strength. Conversely, the COV of tensile strain capacity are in the range of 26%-60% except for PVA-ECC 2 and 3, where the robustness of tensile ductility increased (in the form of reduced COV) due to the usage of high volume fly ash (Wang 2005). This general trend – relatively low COV for tensile strength and high COV for tensile strain capacity can also be found in Kanakubo (2006). This further confirmed the rationale of quality control for the tensile strain capacity instead of tensile strength.

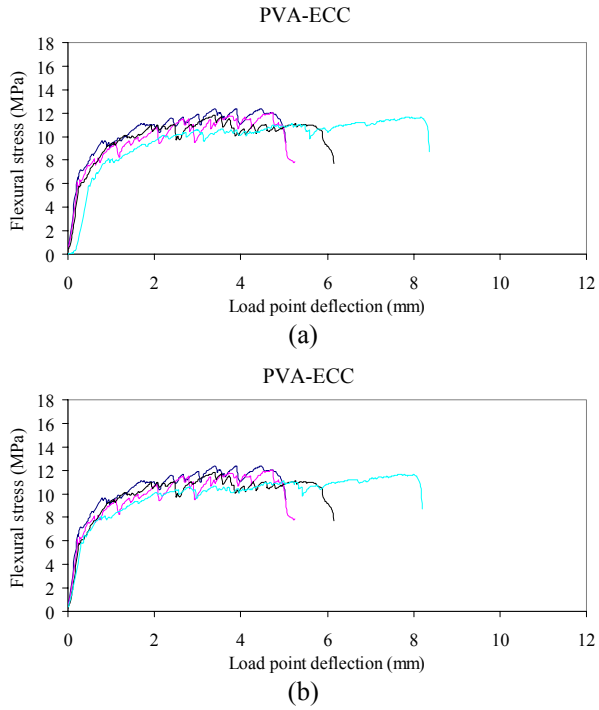

Fig. 11 Experimental flexural stress – load point deflection relation for PVA-ECC 1 (a) before and (b) after correction of the initial loading stage.

The flexural stress-load point deflection curves for PVA-ECC 1 were shown in **Fig. 11**. If the specimen was not fully contacted with the test apparatus, the initial loading stage may show unrealistic low stiffness in some case as shown in **Fig. 11 (a)**. This can be easily corrected by discounting this part of deflection from the load point deflection, as revealed in **Fig. 11 (b)**. The initial deflection with low stiffness, if any, is typically less than 0.2 mm, comprising of less than 5% of the deflection capacity.

Similar to PVA-ECC1 in **Fig. 11**, PVA-ECC 2 and 3 also show typical deflection hardening behavior under FPBT, with the bottom surface of the specimens after bending test shown in **Fig. 12**. More and more saturated microcrack is revealed from PVA-ECC 1 to 3, along with gradual increase of deflection capacity (**Table 7**).

The modulus of rupture for PVA-ECC 1-3 ranges from 10-12 MPa, about 2.4-3.0 times that of their first cracking strength. This is consistent with the finding of Maalej and Li (1994) that this ratio should be about 2.7 for elastic-perfectly plastic material (for tensile portion of beam), such as the PVA-ECCs investigated in this study.

Fig.12 Beam bottom surface shown increasingly saturated microcracks after bending test for PVA-ECC 1-3 (Microcracks are magnified with thick pen for the constant moment span length only).

5. Validation and verification of the proposed method

To validate the proposed inverse method, the deflection capacity obtained from FPBT is converted to tensile strain using Equations (4) and (5) (derived for the same beam size as used in the FPBT experiments) and then compared with tensile strain capacity obtained directly from uniaxial tensile test for PVA-ECC 1-3. As revealed in **Table 7** and **Fig. 13**, the tensile strain capacity derived from FPBT predicts the uniaxial tensile test results with reasonable accuracy, with less than 20% difference. This agreement demonstrates the validity of the proposed inverse method.

To further verify the proposed UM method, comparison between UM method and JCI method was conducted based on JCI round robin test data (Kanakubo 2006). As mentioned previously, bending test results from JCI round robin test are presented in the form of moment –curvature relation. To facilitate the comparison, the curvature capacity can be converted to tensile strain capacity using Equations (6) and (7) in UM method. Within the JCI method, the tensile strain capacity is obtained by solving following equations (JCI-S-003-2005):

$$\varepsilon_{tu,b} = \phi_u \cdot D \cdot (1 - x_{nl}) \tag{8}$$

$$x_{nl}^3 + 3x_{nl}^2 - 12m^* = 0 \tag{9}$$

$$m^* = \frac{M_{\max}}{E \cdot \phi_u \cdot B \cdot D^3} \tag{10}$$

where $\varepsilon_{tu,b}$ is the predicted tensile strain capacity (%); ϕ_u is the curvature capacity (1/mm), which can be calculated from two LVDTs measurements (**Fig. 9 (b)**); D is depth of the test specimen (=100 mm); x_{nl} is the ratio of the distance from compressive edge (extreme compression fiber) to neutral axis over depth of test specimen, which needs to be solved from Equation (9); $M_{\max}$ is maximum moment $(N \cdot mm)$; E is the static modulus of elasticity (N/mm^2); B is the width of test specimen (100 mm). For more details, readers are referred to the Appendix to JCI-S-003-2005.

As shown in **Table 8** and **Fig. 14**, predictions based on both the UM method and the JCI method reveal comparable results with those from uniaxial tensile tests. Furthermore, the UM method shows slightly smaller discrepancy with the uniaxial tensile test result (**Table 8**) based on limited data. The consistency between the UM method and the JCI method and verification by independent JCI round robin test data further demonstrate the validity of the proposed UM method.

The advantage of the UM method over the JCI method lies in its simplicity, both in the experiment and data interpretation phases. In the experiment phase, the UM method only requires machine displacement to be measured. This is not the case for the JCI method, where complicated setup such as LVDTs is needed to measure curvature, as revealed in **Fig. 9 (a)** and **(b)**. In

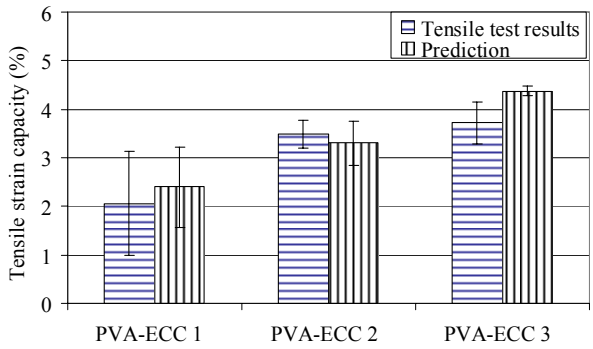

Fig. 13 Comparison of tensile strain capacity from UTT test with prediction from proposed UM method for different PVA-ECCs.

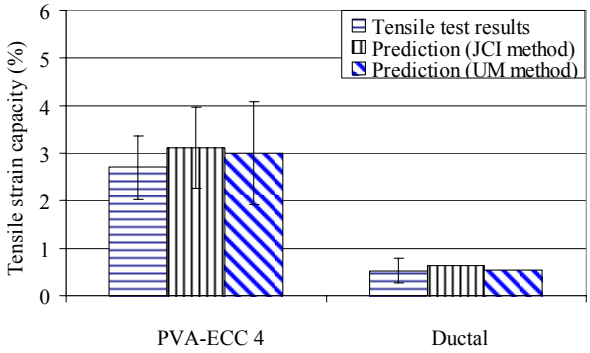

Fig. 14 Comparison of tensile strain capacity from UTT with predictions from JCI method and proposed UM method for different SHCCs. (Experimental data for both UTT and FPBT are from JCI round robin test and only two FPBT specimens were reported for Ductal.)

Table 8 Comparison between uniaxial tensile test results with predictions based on the JCI method and the UM method.

	Tensile strain capacity from UTT (%)	Curvature Capacity from FPBT (μ/mm)	Predicted tensile strain capacity (JCI method) (%)	Predicted tensile strain capacity (UM method) (%)
PVA-ECC 4	2.7±0.7	349.2±96.3	3.1±0.9 (15)	3.0±1.1 (11)
Ductal	0.5±0.3	85.0*	0.6* (20)	0.5* (0)

Note: *: Only two bending specimens were reported. The number in parenthesis is the difference (in percentage) between the predictions and test results from uniaxial tensile test.

the data interpretation phase, the UM method only needs a simple master curve or linear equation to convert deflection capacity directly into tensile strain capacity, while the JCI method requires relatively complicated procedures (solving cubic equation) to obtain tensile strain capacity. Considering the large amount of specimens needed to be tested during construction, the UM method seems to be more suitable for quality control purpose due to its simplicity, efficiency and reasonable accuracy.

6. Conclusions

To facilitate the quality control of the strain hardening cementitious composites on site, a simplified inverse method is proposed to covert the deflection capacity from simple beam bending test to tensile strain capacity through linear transformation. The linear transformation (in the form of master curves) is derived from parametric study with a wide range of parametric values of material tensile and compressive properties based on a theoretical model. This proposed method has been experimentally validated with uniaxial tensile test results with reasonable agreement. In addition, this proposed method compares favorably with the JCI method in accuracy, but without the associated complexity.

The following specific conclusions can be drawn from this study:

1. A simple inverse method has been successfully developed to derive tensile strain capacity of SHCC from beam bending deflection capacity by using a master curve. This method is expected to greatly ease the on-site quality control for SHCC in terms of much simpler experiment setup requirement (compared with both UTT and the JCI inverse method) and data interpretation procedure (compared with the JCI method), yet with reasonable accuracy (within 20%);
2. The master curve features simple linear transformation with a narrow band width. The master curve decouples the dependence of tensile strain capacity on the moment capacity in contrast with the JCI method where tensile strain capacity is dependent on both curvature capacity and moment capacity. Therefore, this method allows simple linear equations (Equation (4) and (5)) to be used for easy data interpretation;
3. A linear relation between the deflection capacity and the tensile strain capacity is observed based on parametric studies. It has been shown that this linear relation is closely related to the fact that the neutral axis of the SHCCs under bending rapidly approaches the extreme compression fiber and quickly stabilizes (the plateau distance from extreme tension fiber to neutral axis is about 90% of the beam depth);
4. All linear curves relating tensile strain capacity and deflection capacity lie in a narrow band regardless of actual material properties. This suggests that beam deflection capacity is most sensitive to tensile strain capacity for a given FPBT geometric dimensions, and much less sensitive to other properties such as compressive strength, Young's Modulus, etc. This could be explained by the fact that the distance from extreme tension fiber to neutral axis stabilizes to about 90% of the beam depth for all SHCCs with different material properties.

It should be noted that the following assumptions are made when the proposed UM method is used: (a) The tested material is truly a strain hardening type; (b) The major target for quality control for this material is tensile ductility; and (c) For this method to be most effective, a standardized beam with fixed geometric dimensions should be agreed upon by the user community.

Acknowledgements

The authors thank the Michigan Department of Transportation, and the National Science Foundation for funding portions of this research (CMS-0223971, CMS-0329416).

References

JCI-S-003-2005. (2005). "Method of test for bendingmoment–curvature curve of fiber reinforced cementitious composites." Japan Concrete Institute Standard, 7.

Kanakubo, T. (2006). "Tensile characteristics evaluation method for DFRCC." *Journal of Advanced Concrete Technology*, 4 (1), 3-17.

Kanda, T., Kanakubo, T., Nagai, S. and Maruta, M. (2006). "Technical consideration in producing ECC Pre-cast structural element." *Proceedings of*

International RILEM workshop on HPFRCC in structural applications, Published by RILEM SARL, 229-242.

Kanda, T., Saito, T., Sakata, N. and Hiraishi, M. (2002). "Fundamental properties of direct sprayed ECC." *Proceedings of the JCI International Workshop on Ductile Fiber Reinforced Cementitious Composites (DFRCC) - Application and Evaluation (DRFCC-2002)*, Takayama, Japan, 133-142.

Li, V. C. (2005). "Engineered cementitious composites." *Proceedings of ConMat'05*, Vancouver, Canada, August 22-24, CD-documents/1-05/SS-GF-01_FP.pdf.

Li, V. C. (2004). "Strategies for high performance fiber reinforced cementitious composites development." *Proceedings of International Workshop on Advances in Fiber Reinforced Concrete*, Bergamo, Italy, 93-98.

Li, V. C. (2003). "On engineered cementitious composites (ECC) – A review of the material and its applications." *Journal of Advanced Concrete Technology*, 1 (3), 215-230.

Li, V. C., Wang, S. and Wu, C. (2001). "Tensile strain-hardening behavior of PVA-ECC." *ACI Materials Journal*, 98 (6), 483-492.

Li, V. C. and Kanda, T. (1998). "Engineered cementitious composites for structural applications." Innovations Forum in ASCE, *Journal of Materials in Civil Engineering*, 66-69.

Li, V. C. (1993). "From micromechanics to structural engineering--The design of cementitous composites for civil engineering applications." *JSCE Journal of Structural mechanics and Earthquake Engineering*, 10(2), 37-48.

Maalej, M. and Li, V. C. (1994). "Flexural/tensile strength ratio in engineered cementitious composites." *ASCE Journal of Materials in Civil Engineering*, 6(4), 513-528.

Naaman, A. E. and Reinhardt, H. W. (1996). "Characterization of high performance fiber reinforced cement composites (HPFRCC)." in *High Performance Fiber Reinforced Cementitious Composites*, RILEM Proceedings 31, Eds. A. E. Naaman and H. W. Reinhardt, 1-23.

Ostergaard, L., Walter, R. and Olesen, J. F. (2005). "Method for determination of tensile properties of engineered cementitious composites (ECC)." *Proceedings of ConMat'05*, Vancouver, Canada.

Stang, H. and Li, V. C. (2004). "Classification of fiber reinforced cementitious materials for structural applications." *Proceedings of BEFIB*, Varenna, Lake Como, Italy, 197-218.

Wang, S. and Li, V. C. (2004). "Tailoring of pre-existing flaws in ECC matrix for saturated strain hardening." *Proceedings of FRAMCOS-5*, Vail, Colorado, U S A, 1005-1012.

Wang, S. (2005). *Micromechanics based matrix design for engineered cementitious composites*, PhD Thesis, Univ of Michigan, Ann Arbor, MI, 222.